

The effect of titanium and phosphorus on ferric/ferrous ratio in silicate melts: an experimental study

Alexander Borisov · Harald Behrens ·
Francois Holtz

Received: 22 April 2013 / Accepted: 19 September 2013 / Published online: 6 October 2013
© Springer-Verlag Berlin Heidelberg 2013

Abstract The effect of TiO_2 and P_2O_5 on the ferric/ferrous ratio in silicate melts was investigated in model silicate melts at air conditions in the temperature range 1,400–1,550 °C at 1-atm total pressure. The base composition of the anorthite–diopside eutectic composition was modified with 10 wt % Fe_2O_3 and variable amounts of TiO_2 (up to 30 wt %) or P_2O_5 (up to 20 wt %). Some compositions also contained higher SiO_2 concentrations to compare the role of SiO_2 , TiO_2 , and P_2O_5 on the $\text{Fe}^{3+}/\text{Fe}^{2+}$ ratio. The ferric/ferrous ratio in experimental glasses was analyzed using a wet chemical technique with colorimetric detection of ferrous iron. It is shown that at constant temperature, an increase in SiO_2 , TiO_2 , and P_2O_5 content results in a decrease in the ferric/ferrous ratio. The effects of TiO_2 and SiO_2 on the $\text{Fe}^{3+}/\text{Fe}^{2+}$ ratio was found to be almost identical. In contrast, adding P_2O_5 was found to decrease ferric/ferrous ratio much more effectively than adding silica. The results were compared with the predictions from the published empirical equations forecasting $\text{Fe}^{3+}/\text{Fe}^{2+}$ ratio. It was demonstrated that the effects of TiO_2 are minor but that the effects of P_2O_5 should be included in models to better describe ferric/ferrous ratio in phosphorus-bearing silicate melts. Based on our observations, the determination of the prevailing $f\text{O}_2$ in magmas

from the $\text{Fe}^{3+}/\text{Fe}^{2+}$ ratio in natural glasses using empirical equations published so far is discussed critically.

Keywords Ferric/ferrous ratio · Silicate melt · TiO_2 · P_2O_5 · Experiment

Introduction

Iron in silicate melts is stable in two oxidation states, Fe^{3+} and Fe^{2+} , with the first species prevailing at high $f\text{O}_2$ and the second one at low $f\text{O}_2$ values. The ferric/ferrous equilibrium in melts can be described by the reaction:



with the reaction constant:

$$K = a_{\text{FeO}_{1.5}} / (a_{\text{FeO}} \cdot f\text{O}_2^{1/4}) \\ = (X_{\text{FeO}_{1.5}}/X_{\text{FeO}}) \cdot (\gamma_{\text{FeO}_{1.5}}/\gamma_{\text{FeO}}) / f\text{O}_2^{1/4} \quad (2)$$

where a_i and γ_i are the activities and activity coefficients, respectively, of iron oxides in silicate melts, X_i refers to the mole fraction on oxide basis, and $f\text{O}_2$ is the oxygen fugacity. The Eq. (2) may be further converted into

$$\log(X_{\text{FeO}_{1.5}}/X_{\text{FeO}}) = \frac{1}{4} \log f\text{O}_2 + \log K - \log(\gamma_{\text{FeO}_{1.5}}/\gamma_{\text{FeO}}) \quad (3)$$

In this equation, the coefficient (k) at $\log f\text{O}_2$ is equal to 1/4 in an ideal case, when $\gamma_{\text{FeO}_{1.5}}/\gamma_{\text{FeO}}$ is approximately constant in the $f\text{O}_2$ range under consideration. However, small deviations of k from the ideal value have been reported and are the subject of discussion (e.g., Kress and Carmichael 1988, 1991; Jayasuriya et al. 2004; Borisov 2010).

At constant T - $f\text{O}_2$ conditions, $\log(X_{\text{FeO}_{1.5}}/X_{\text{FeO}})$ must be proportional to $\log(\gamma_{\text{FeO}_{1.5}}/\gamma_{\text{FeO}})$ in the silicate liquid,

Communicated by J. Hoefs.

A. Borisov (✉)
Institute of Geology of Ore Deposits, Petrography, Mineralogy
and Geochemistry, Russian Academy of Sciences, Staromonety
35, 109017 Moscow, Russia
e-mail: aborisov@igem.ru

A. Borisov · H. Behrens · F. Holtz
Institut für Mineralogie, Leibniz Universität Hannover,
Callinstrasse 3, 30167 Hannover, Germany

which reflects the compositional dependence of the ferric/ferrous ratio. In a simple case such a dependence may be approximated as a linear function of the mole fractions of the main oxide component in silicate melts (SiO_2 , Al_2O_3 , MgO , CaO , Na_2O , and K_2O), $\sum d_i X_i$, where d_i and X_i are empirical coefficients and mole fractions of individual oxides in the melt, respectively. This results in empirical equations in which $\text{Fe}^{3+}/\text{Fe}^{2+}$ ratio is a function of T , $f\text{O}_2$, and melt composition in the form (e.g., Sack et al. 1980; Kilinc et al. 1983):

$$\ln(X_{\text{Fe}_2\text{O}_3}/X_{\text{FeO}}) = k \cdot \ln f\text{O}_2 + h/T + \sum d_i X_i + c \quad (4)$$

where T is in K , and k , h , and c are constants. The type (4) empirical equations are important from two points of view:

1. For given experimental or suggested natural T - $f\text{O}_2$ conditions, such equations allow to recalculate Fe^{3+} and Fe^{2+} species in glasses in which only the total Fe (Fe_t) is known, typically determined with EPMA. For example, the determination of the Fe–Mg partition coefficient between olivine and melt (Roeder and Emslie 1970; Toplis 2005) requires prior calculation of the proportions $\text{Fe}^{3+}/\text{Fe}_t$. The different size and charge of Fe^{3+} and Fe^{2+} imply that physical and chemical properties of silicate melts are affected by the $\text{Fe}^{3+}/\text{Fe}^{2+}$ ratio and also explain why the distribution of Fe^{3+} and Fe^{2+} is different in melts and coexisting crystalline phases.
2. The $\text{Fe}^{3+}/\text{Fe}^{2+}$ ratio, similar to some other redox pairs, may be used for the estimation of the redox conditions of magmas and of the regions of magma generation. The best example is an estimation of $f\text{O}_2$ of the mantle from which mid-ocean ridge basalt (MORB) was derived (Christie et al. 1986; Nikolaev et al. 1996; Bézos and Humler 2005; Cottrell and Kelley 2011, 2013). The approach is based on the determination of $\text{Fe}^{3+}/\text{Fe}_t$ ratios in MORB glasses by applying empirical equations such as Eq. (4). Christie et al. (1986) conducted wet chemical analyses of 78 hand-picked MORB glasses, applied Kilinc's et al. (1983) equation and estimated $f\text{O}_2$ to be 1–2 log units below the quartz–fayalite–magnetite buffer (QFM). Cottrell and Kelley (2011) analyzed 103 MORB glasses with micro-X-ray absorption near-edge structure (μ -XANES), applied Kress and Carmichael's (1991) equation, and estimated $f\text{O}_2$ to be around QFM. Note that the reason for such a large discrepancy between these two $f\text{O}_2$ estimations is primarily due to very different average $\text{Fe}^{3+}/\text{Fe}_t$ ratios found for MORB glasses (0.07 ± 0.03 in the first case and 0.16 ± 0.01 in the second one), because of the possible presence of microcrystals in the samples analyzed by wet chemistry. However, using different equations may also affect $f\text{O}_2$

determination. For example, Nikolaev et al. (1996) re-estimated $f\text{O}_2$ in fourteen MORB glasses already analyzed by Christie et al. (1986) using their own calibration, and $f\text{O}_2$ was found to be higher by 0.55 log unit in average than reported in the previous paper.

In most empirical equations proposed so far to model the link between $\text{Fe}^{3+}/\text{Fe}^{2+}$ ratio and $f\text{O}_2$, oxides such as TiO_2 , MnO , Cr_2O_3 , and P_2O_5 are ignored because they “have very low concentrations in silicate liquids and are often not reported in the published data” (Sack et al. 1980, p. 373). However, the effects of such minor components on ferric/ferrous ratio may be not negligible.

Two of these minor components such as Mn and Cr occur in silicate melts in different valence states, Mn^{3+} and Mn^{2+} and Cr^{6+} , Cr^{3+} and Cr^{2+} , depending on $f\text{O}_2$ (e.g., Johnston 1965; Schreiber and Haskin 1976; Pretorius et al. 1992; Schreiber et al. 1996). The investigation of the effect of these oxides on ferric/ferrous ratio is not a trivial task, because of the possible exchange of electrons between redox pairs during quenching of melts into glasses (e.g., Lahiri et al. 1974; Rüssel 1989; Borisov 2013). The study of such equilibria in situ at high temperature may be an option, but is technically difficult (Berry et al. 2003). The two other minor components such as Ti and P exist only in one valence state and Ti^{4+} and P^{5+} in silicate melts at $f\text{O}_2$ conditions typically used in experiments on ferric/ferrous determination (from air to about QFM-2). Trivalent titanium in silicate melts is present in reasonable amount only at $f\text{O}_2$ below iron–wüstite (IW) buffer conditions (Johnston 1965; Schreiber et al. 1978; Borisov 2012). Phosphorus as phosphide ion (P^{3-}) was found in slags under strongly reducing conditions, more than 9 orders of magnitude below IW (Momokawa and Sano 1982). Due to the lacking redox variation of Ti and P under oxidizing to intermediate conditions (up to iron–wüstite buffer), the effect of these elements on ferric/ferrous ratio in silicate melts can be studied by “classical techniques,” i.e., by analyzing quenched samples (glasses).

TiO_2 is one of the main components of lunar high-Ti basalts, which were collected in the Apollo 11 and 17 missions, with concentrations up to 15 wt % (BVSP, 1981). Terrestrial magmatic rocks are usually poor in titania, but in some cases they may contain up to 5 wt % (e.g., Pik et al. 1998). Phosphorus content in primitive mantle is estimated to be very low (86 ppm, Palme and O'Neil 2003). However, being highly incompatible, P content may increase in a melt during partial melting and fractional crystallization processes. The main P-bearing phase, apatite, has high solubility in high-temperature basaltic silicate melts (Watson 1980), and P_2O_5 content in such melts may reach a few weight percents before the saturation with apatite (up to 2 wt % P_2O_5 in Fe-rich basaltic systems, e.g., Auwera and Longhi 1994).

Even such small P_2O_5 contents may be essential in affecting iron redox ratio but, in the absence of experimental calibrations, such effects are not well constrained. Jayasuriya et al. (2004) stressed “the extraordinarily high” ability of P_2O_5 to decrease Fe^{3+}/Fe^{2+} . Mysen (1992) found two opposite trends in changing ferric/ferrous ratio by diluting an initial Ca silicate melt either with P_2O_5 or with $Ca_3(PO_4)_2$. At last, Gwinn and Hess (1993) revealed a significant increase in Fe^{3+}/Fe^{2+} with the addition of P in very silicic melts with SiO_2 concentrations up to 78 wt %.

Although the effect of melt composition on the Fe^{3+}/Fe^{2+} ratio is small in comparison with the effects of temperature and, especially, oxygen fugacity, it cannot be ignored. To clarify the compositional dependence of the ferric/ferrous ratio in silicate melts, investigations in rather simple systems have been conducted, e.g., Na_2O – FeO – Fe_2O_3 – SiO_2 (Lange and Carmichael 1989), K_2O – FeO – Fe_2O_3 – SiO_2 (Tangeman et al. 2001), and CaO – FeO – Fe_2O_3 – SiO_2 (Kress and Carmichael 1989). Alternatively, natural melts may be modified by adding the components of interest. For example, Thornber et al. (1980) modified an initial diabase composition by increasing Al_2O_3 up to 28.7 wt %, CaO up to 24.3 wt %, K_2O up to 7.6 wt %, which are the concentrations well above that of typical basaltic melts. One may argue that the effect on Fe^{3+}/Fe^{2+} may be different for low and high amounts of components. However, often variation over a large compositional range is required to properly resolve such effects. Following this approach, we have added up to 30 wt % TiO_2 and up to 20 wt % P_2O_5 to a haplobasaltic melt to quantify the effect of these components on the redox state of iron.

Experimental procedure

A synthetic iron-free melt of diopside–anorthite eutectic composition (DA) was chosen as the base composition for the experiments. This composition was modified by adding about 10 wt % Fe_2O_3 (total iron expressed as Fe_2O_3) and different amounts of TiO_2 or P_2O_5 to obtain two sets of melt compositions: DAFT series (DAF, DAFT10, DAFT20, and DAFT30) with a total formula of $10Fe_2O_3 \cdot xTiO_2 \cdot (90-x)DA$ and DAFP series (DAF, DAFP05, DAFP10, DAFP15, and DAFP20) with a total formula of $10Fe_2O_3 \cdot xP_2O_5 \cdot (90-x)DA$. Some Ti-containing mixtures were additionally modified by adding silica (DAFST series: DAFS, DAFST15, and DAFST25) with a total formula of $10Fe_2O_3 \cdot xTiO_2 \cdot (90-x) \cdot (0.5DA \cdot 0.5SiO_2)$. One P-containing mixture (DAFP10) was also modified by adding silica (marked as DAFSP08). In all cases, the two-digit numbers in the mixture label denote the rough amount of TiO_2 or P_2O_5 (wt %) and x in formulas refer to wt % of the respective components.

The experiments were conducted in a one-atmosphere vertical tube furnace with the loop technique (e.g., Donaldson et al. 1975). Platinum wire (0.125 mm thick and 99.9 % pure, Chempur[®]) was used to prepare loops about 2 or 3 mm in diameter. Silicate powder mixed with weak polyvinyl alcohol–water solution was inserted into the loops that were then suspended on the sample holder and transferred into the furnace. The investigated temperature range was 1,400–1,550 °C. Temperatures were determined with a Pt/PtRh₁₀ thermocouple that was calibrated against the melting point of Au (1,064 °C) and expected to be accurate within ± 2 °C. All experiments were conducted in air.

Two sample sizes were used in this study: 2-mm loops with average sample weight of about 14 mg for preliminary investigations of phosphorus loss from DAFP10 composition (Table 1) and 3-mm loops with average sample weight of about 30 mg for the main series of experiments (Table 2). In the last case, up to 7 samples of different composition were simultaneously placed into the furnace at a given temperature.

In order to determine equilibration times, experimental series with different run duration were conducted with basic (DAF) and more silicic (DAFS) compositions at 1,500 °C. Although redox equilibrium was found to be reached quickly (see below), most of the experiments with Ti-containing compositions were carried out with relatively long duration (e.g., 70 h at 1,450 °C).

The loss of phosphorus from the melts even at air conditions (see below) forced us to reduce experimental duration with P-containing compositions to a minimum needed to reach equilibrium Fe^{3+}/Fe^{2+} ratio. However, DAFSP08 composition was found to be very viscous in comparison with all other mixtures and thus potentially to be most problematic in reaching equilibrium. Thus, a few longer runs with DAFSP08 were performed to have a time series at 1,500 °C.

After the experiments, the samples were quenched by quickly withdrawing the sample holder from the furnace. The small weight of the loop samples (30–35 mg) guarantees fast quenching. The samples were then crushed, and at least two small glass fragments of each sample were mounted in epoxy, polished, and carbon-coated for electron microprobe analysis (EMPA).

Bulk compositions of experimental glasses were determined by EMPA using a Cameca SX100. Conditions of measurements were 15 keV accelerating voltage, 15 nA beam current, 10 s counting time, and focused beam. At least twenty points were analyzed in each glass sample, and the average composition of the run products is given in Table 2.

The ferric/ferrous ratio in experimental glasses was analyzed using a wet chemical technique, based on the

Table 1 Phosphorus loss from samples at oxidizing (air) and reducing (IW) conditions

Duration (h)	T °C	P ₂ O ₅ wt %	er. wt %	Sample weight (mg)
DAFP10 series, air (present study)				
Initial		10.6	0.1	
2	1,500	10.2	0.1	10.8
7	1,500	9.8	0.1	15.2
17.2	1,500	8.8	0.1	13.9
2	1,450	10.4	0.1	12.2
7	1,450	10.1	0.1	13.6
15.5	1,450	9.5	0.1	13.1
66	1,450	7.8	0.1	15.0
DAP ^a series, IW (Borisov, unpublished data)				
Initial		12.9	0.3	
3	1,450	10.9	0.3	15.2
8	1,450	9.1	0.2	12.6
15	1,450	7.3	0.2	12.6
24	1,350	10.6	0.2	18.1
53	1,350	8.6	0.3	16.2
71	1,350	8.1	0.1	17.2

^a DAP = DA + Ca₂P₂O₇, IW are approximately iron–wustite buffer conditions defined by CO/CO₂ gas mixture

colorimetric method of Wilson (1960) and modified following the procedure given by Schuessler et al. (2008). In brief, the analytical procedure is as follows: 5–7 mg of powdered sample was weighed into a 15-mL Teflon beaker containing 1 mL of an ammonium vanadate solution dissolved in sulfuric acid (5 M H₂SO₄). After the addition of 0.5–1 mL concentrated HF, the beaker was tightly sealed and left overnight at room temperature. It is assumed that V⁵⁺ in vanadate solution oxidizes Fe²⁺ as soon as it is released from the sample according to the reaction:



with V⁴⁺ in solution being much more resistant to oxidation when compared to Fe²⁺. After sample dissolution, 5 mL saturated boric acid solution was added to neutralize the excess HF. The content of the beaker was then quantitatively transferred into a 100-mL volumetric flask, containing 10 mL ammonium acetate solution and 5 mL 2:2' bipyridyl solution, and the remaining volume was filled with distilled water. The ammonium acetate buffer adjusted the pH value to about 5, which brings the reaction (5) to the left and regenerates Fe²⁺ from Fe³⁺. The complex of Fe²⁺ with 2:2' bipyridyl shows an intensive absorption band at about 523 nm. Measurements of Fe²⁺ and Fe_{tot} were taken with Shimadzu UV-1800 spectrometer on the same solution before and after adding 5–10 mg solid hydroxylamine hydrochloride to an aliquant of about 10 mL. This reducing

agent converts all Fe³⁺ into Fe²⁺. The advantage of such modification is that uncertainties in ferric/ferrous ratios arise mainly from the spectrometric measurements, whereas weighing and dilution errors cancel out.

All experimental glasses were analyzed in three sessions (Table 2). An in-house standard PU-3 (see Schuessler et al. 2008 for details) with known Fe²⁺ and Fe_t was included in every session. The Fe³⁺/Fe²⁺ ratios were found to be 1.47 ± 0.08, 1.53 ± 0.08, and 1.52 ± 0.08, which are identical within error limits to the values 1.60 ± 0.11 (1σ for the average of 33 measurements collected over a time period of about 1 year) determined by Schuessler et al. (2008).

Results

Phosphorus evaporation from experimental samples at high temperatures

The results of the phosphorus loss from the melts of DAFP10 composition at air conditions are given in Table 1. Previous studies (Borisov, unpublished data) of phosphorus evaporation from the melts of DAP composition (DAP = Diopside–Anorthite eutectic composition + Ca₂P₂O₇) demonstrated a severe P loss at IW buffer conditions adjusted by CO/CO₂ gas mixture, and the results are also shown in Table 1. Note that the errors of P₂O₅ contents given in Table 1 are standard deviations for an average of ten measurements, typically made along a profile across the whole sample. The low values of these errors reflect relatively homogeneous phosphorus content even in samples that suffered substantial loss of phosphorus. One of the reasons of such homogeneity can be convection, which can occur in the melt droplets (Borisov 2001). In addition to *T*-*f*O₂ conditions, the sample size (surface exposed to air or gas flux) and melt composition may also affect the extent of P loss by evaporation. Considering that the compositions are rather similar (DA as a base) and that the samples have a similar weight (13.4 ± 1.5 mg for DAFP10 vs. 15.3 ± 2.3 mg for DAP samples), we will discuss them together (Fig. 1).

Run duration and redox conditions are found to be most critical for P loss (Fig. 1). At 1,450 °C and IW buffer conditions, about 45 % of initial P content was lost from the sample after 15 h. At the same temperature in air conditions during similar duration, only 10 % of phosphorus was lost. The temperature of experiments is also important. For example, at air condition and similar duration of 15–17 h, a temperature increase from 1,450 to 1,500 °C results in an increase in P loss from 10 to 17 %.

The phosphorus loss at constant *T*-*f*O₂ conditions seems to be a quadratic function of the run duration τ (*h*). For example, at air conditions and 1,450 °C, the phosphorus

Table 2 Experimental conditions, microprobe composition (wt %) of experimental glasses and ferric/ferrous ratios determined by wet chemical colorimetric analyses

	Sample	T °C	Duration (h)	SiO ₂	TiO ₂	Al ₂ O ₃	Fe ₂ O ₃	MgO	CaO	P ₂ O ₅	Total	Fe ³⁺ /Fe ²⁺
1	DAF-5	1,502	24	45.49	0.02	14.08	9.75	9.11	21.22	–	99.67	1.871
2	DAFT10-5	“	“	40.96	9.10	12.54	9.35	8.08	18.88	–	98.91	1.75
3	DAFT20-5	“	“	35.12	19.46	10.73	9.59	7	16.26	–	98.16	1.67
4	DAFT30-5	“	“	30.47	28.14	9.42	9.6	6.11	14.29	–	98.04	1.60
5	DAFS-5	“	“	66.25	0.01	7.57	9.99	4.82	11.41	–	100.05	1.42
6	DAFST15-5	“	“	55.93	14.23	6.22	9.33	4.01	9.48	–	99.2	1.28
7	DAFST25-5	“	“	48.33	24.61	5.39	9.67	3.44	8.3	–	99.74	1.20
8	DAF-6	1,503	14.5	45.45	0.03	14.1	9.67	9.11	21.35	–	99.7	1.90
9	DAFS-6	“	“	66.8	0.01	7.61	9.66	4.82	11.34	–	100.24	1.41
10	DAF-7	1,503	8	45.41	0.01	14.03	9.64	9.06	21.36	–	99.5	1.93
11	DAFS-7	“	“	67.01	0	7.48	9.45	4.84	11.22	–	100.01	1.40
12	DAF-9	1,501	2	45.53	0.02	14.19	9.89	9.12	21.4	–	100.15	1.87
13	DAFS-9	“	“	64.35	0	7.82	10.84	5.17	11.85	–	100.23	1.41
14	DAF-10	1,451	70	45.58	0.02	14.23	9.59	9.08	21.56	–	100.06	2.551
15	DAFT10-10	“	“	40.54	9.62	12.49	9.47	8.12	18.84	–	99.08	2.43
16	DAFT20-10	“	“	35.05	19.51	10.83	9.47	6.99	16.46	–	98.3	2.27
17	DAFT30-10	“	“	30.44	28.47	9.39	9.5	6.14	14.42	–	98.36	2.12
18	DAFS-10 ^a	“	“	65.82	0.01	7.72	9.58	4.93	11.57	–	99.64	1.87
19	DAFST15-10 ^a	“	“	54.94	14.55	6.38	9.41	4.12	9.61	–	99	1.73
20	DAFST25-10 ^a	“	“	46.33	25.56	5.64	9.88	3.58	8.67	–	99.89	1.62
21	DAF-13	1,400	72	45.64	0.02	14.14	9.56	9.13	21.45	–	99.94	3.17
22	DAFT10-13	“	“	40.9	9.18	12.56	9.34	8.06	18.89	–	98.92	2.99
23	DAFT20-13	“	“	34.96	19.54	10.71	9.48	6.96	16.36	–	98	2.73
24	DAFT30-13	“	“	30.31	28.62	9.39	9.63	6.06	14.28	–	98.3	2.55
25	DAF-30	1,451	9.0	45.52	–	14.13	9.81	9.54	21.33	0.58	100.92	2.31
26	DAFP05-30	“	“	43.11	–	13.40	9.75	9.08	20.16	5.45	100.94	1.86
27	DAFP10-30	“	“	40.81	–	12.65	9.71	8.48	18.96	10.50	101.11	1.47
28	DAFP15-30	“	“	38.43	–	12.00	9.80	7.97	17.80	15.23	101.23	1.18
29	DAFP20-30	“	“	36.81	–	11.40	9.72	7.41	16.66	19.33	101.33	0.98
30	DAF-28	1,501	2.0	45.78	–	14.25	9.73	9.57	21.45	0.31	101.09	1.92
31	DAFP05-28	“	“	43.47	–	13.48	9.75	9.03	20.22	5.38	101.32	1.55
32	DAFP10-28	“	“	40.81	–	12.68	9.75	8.52	18.94	10.57	101.27	1.23
33	DAFP15-28	“	“	38.46	–	12.03	9.70	7.96	17.71	15.61	101.46	0.99
34	DAFP20-28	“	“	35.92	–	11.22	9.64	7.44	16.63	20.54	101.39	0.82
35	DAFSP08-39	1,501	2.0	50.81	–	10.12	9.77	6.75	15.06	8.00	100.51	1.13
36	DAFSP08-40	1,502	4.0	50.88	–	10.18	9.85	6.79	15.16	7.72	100.58	1.15
37	DAFSP08-42	1,502	8.0	51.44	–	10.28	9.73	6.84	15.38	7.15	100.82	1.17
38	DAF-33	1,552	1.08	45.69	–	14.27	9.57	9.54	21.47	0.34	100.89	1.59
39	DAFP05-33	“	“	43.31	–	13.49	9.72	9.06	20.23	5.31	101.11	1.29
40	DAFP10-33	“	“	40.68	–	12.70	9.68	8.52	18.97	10.49	101.04	1.02
41	DAFP15-33	“	“	38.35	–	12.02	9.74	7.93	17.69	15.51	101.24	0.83
42	DAFP20-33	“	“	36.55	–	11.43	9.71	7.30	16.41	19.94	101.35	0.69
43	DAFSP08-41	1,552	1.5	51.10	–	10.10	9.82	6.75	15.08	7.89	100.75	0.99
	DAP initial ^b			38.43	–	12.58	–	7.59	28.74	12.93	100.26	

All series were made at air conditions; “ the charge was melted in the same experimental run as the sample above

^a Samples contain trace silica; Fe₂O₃ refers to the total iron oxide; Fe³⁺/Fe²⁺ was determined in three sessions, denoted by the division of the column in three sections, the error of determination is approximately ±0.08 for all glasses

^b DAP = DA + Ca₂P₂O₇. The composition was used only to study P evaporation at IW buffer conditions (see text for details)

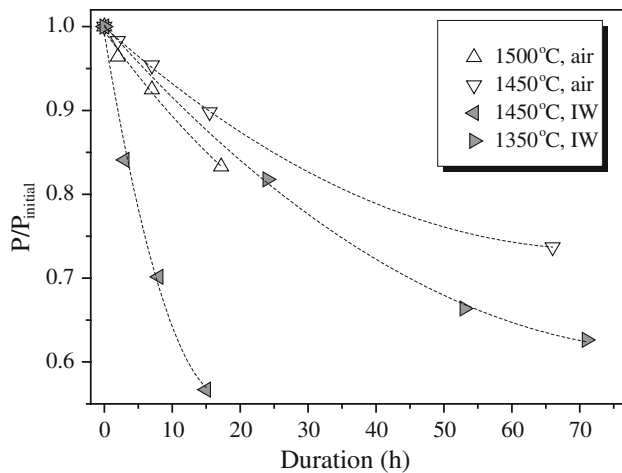


Fig. 1 Effect of temperature and redox conditions on P loss from experimental melts

content can be predicted for the applied experimental setup with following equation ($R^2 = 0.999$):

$$P/P_{\text{ini}} = 1 - 0.00728 \cdot \tau + 4.993 \cdot 10^{-5} \cdot \tau^2 \quad (6)$$

It is emphasized that the phosphorus loss is less problematic in the experiments conducted to determine the $\text{Fe}^{3+}/\text{Fe}^{2+}$ ratio. As it was mentioned above, the samples of the main P series (compositions used for the experiments listed in Table 2) were melted on 3-mm loops and had an average weight of about 30 mg, which is roughly two times higher than that used for the experiments investigating the phosphorus loss. Thus, the phosphorus loss from these samples is smaller. For example, a ~ 30 mg sample DAFP10–30 (1,450 °C, 9 h, see Table 2) contains 10.5 ± 0.1 wt % P_2O_5 , whereas a small sample (~ 15 mg) of the same initial composition melted at the same conditions would contain only 9.9 wt % P_2O_5 according to Eq. (6).

Equilibrium series for the investigation of the $\text{Fe}^{3+}/\text{Fe}^{2+}$ ratio

The results of the time series experiments with the basic DAF and more silicic DAFS compositions are shown on Fig. 2a. The $\text{Fe}^{3+}/\text{Fe}^{2+}$ ratio in samples of the same composition equilibrated for 2, 8, 14.5, and 24 h are the same within 1σ error limits, demonstrating fast achievement of equilibrium between melt and air at 1,500 °C. Additionally, the coincidence of the results in four independent experimental charges of the same composition validates the very good reproducibility of ferric/ferrous determination at least within the same analytical session. Fast equilibration of $\text{Fe}^{3+}/\text{Fe}^{2+}$ was previously found in natural melts equilibrated with air by the loop technique (e.g., <5 h at 1,350 °C, Kilinc et al. 1983).

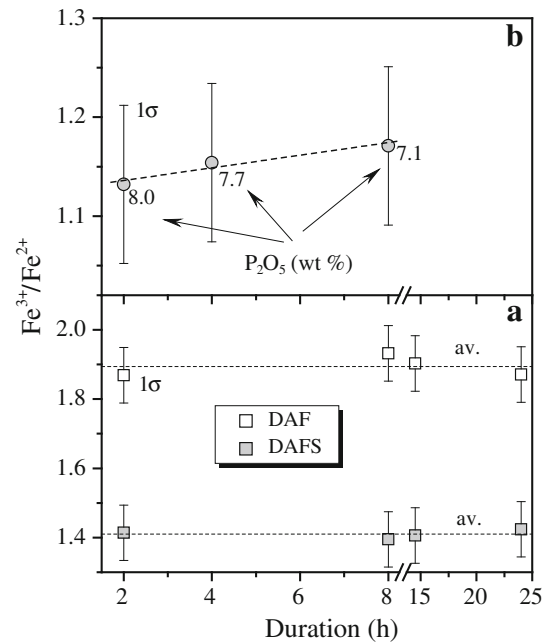


Fig. 2 Effect of equilibration time on ferric/ferrous ratio at 1,500 °C: **a** in basic (DAF) and more silicic (DAFS) melts; **b** in melts of DAFSP08 composition

The results of the time series experiments with the most viscous DAFSP08 composition at 1,500 °C are shown on Fig. 2b. Although the $\text{Fe}^{3+}/\text{Fe}^{2+}$ ratios in samples equilibrated for 2, 4, and 8 h are identical within 1σ error limits, a small trend in increasing the ratio with run duration is evident. Note that one cannot guarantee exactly the same composition in time series because P loss even from large samples at temperature as high as 1,500 °C is not negligible. Indeed, P_2O_5 content decreases from 8.0 wt % for the shortest experiment to 7.1 wt % for longest one. We will further demonstrate that the addition of phosphorus results in an essential decrease in $\text{Fe}^{3+}/\text{Fe}^{2+}$ ratio in silicate melts. It means that P loss should raise this ratio, and slightly different phosphorus content could explain the trend observed on Fig. 2b.

The effect of TiO_2 and P_2O_5 contents on the $\text{Fe}^{3+}/\text{Fe}^{2+}$ ratio

The decrease in $\text{Fe}^{3+}/\text{Fe}^{2+}$ with TiO_2 content is evident for the three investigated temperatures both for basic DAFT and silicic DAFST series (Fig. 3). Note that the $\text{Fe}^{3+}/\text{Fe}^{2+}$ ratio is systematically lower in the more silicic than in the basic samples (data at 1,500 and 1,450 °C) independent from TiO_2 concentration. The comparison of the Ti-free samples, DAF-9 (1,500 °C) and DAFS-10 (1,450 °C) having exactly the same $\text{Fe}^{3+}/\text{Fe}^{2+} = 1.87$ (see Table 2), indicates that increasing silica content in the melt by 20 wt % is equivalent to a temperature increase of 50 °C in affecting the ferric/ferrous ratio.

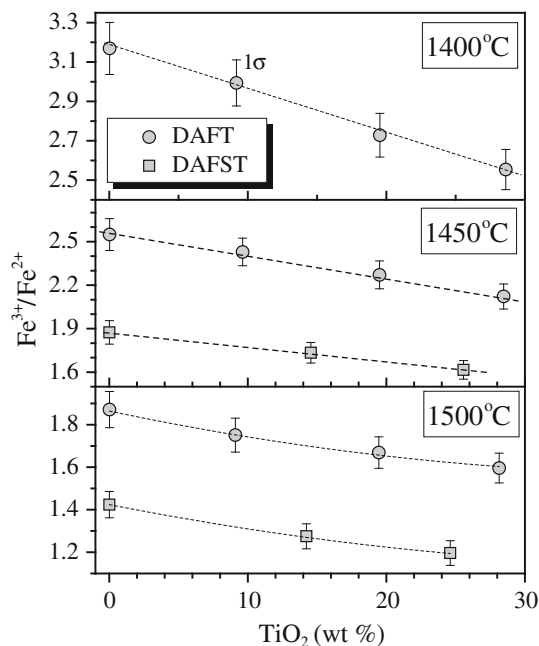


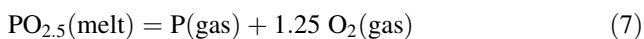
Fig. 3 Effect of TiO₂ on ferric/ferrous ratio in the experimental samples

On Fig. 4, the effect of P₂O₅ on ferric/ferrous ratio in the DAFP series is shown. The decrease in Fe³⁺/Fe²⁺ value upon P addition is intense for all investigated temperatures, about 1.6 times when comparing P-free DAF and DAFP10 (av. 10.5 wt % P₂O₅) compositions and up to 2.3 times when comparing DAF and DAFP20 (av. 19.9 % P₂O₅) compositions.

Discussion

Phosphorus evaporation from silicate melts

The phosphorus behavior is similar to that of the sodium loss from the melt at high temperatures and low *f*O₂ values, which is a main problem of the loop technique and which is well documented (e.g., Corrigan and Gibb 1979; Tsuchiyama et al. 1981; Sugawara 1999). Following Tsuchiyama et al. (1981), who suggested sodium evaporation as metallic species, we suggest a similar reaction for the phosphorus loss from the melt:



with the following equilibrium constant:

$$K_7 = f_P \cdot f_{O_2}^{1.25} / a_{PO_{2.5}} \tag{8}$$

where *f*_P, *f*O₂, and *a*_{PO_{2.5}} are the fugacities of P and O₂ in a vapor phase and the activity of PO_{2.5} in silicate melt, respectively. The Eq. (8) may be further converted into

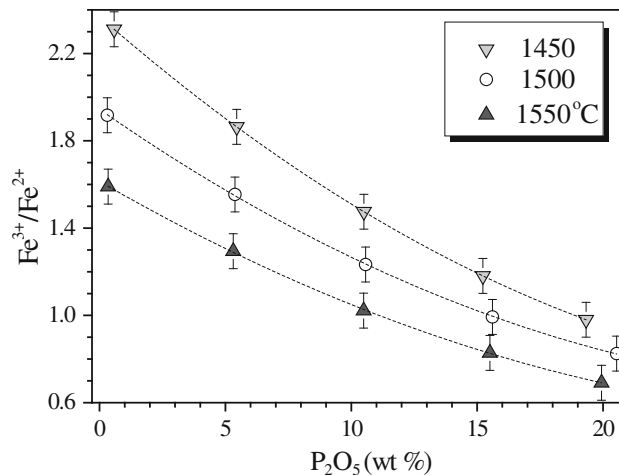


Fig. 4 Effect of P₂O₅ on ferric/ferrous ratio in the experimental samples of DAFP series

$$\log f_P = -1.25 \log f_{O_2} + \log a_{PO_{2.5}} + K_7 \tag{9}$$

Thus, at constant temperature, P fugacity (and, therefore, P loss) will increase with decreasing *f*O₂ and increasing P content in a sample.

Note that the phosphorus loss at air conditions found in the present study is substantial but not as crucial as was revealed by Kilinc et al. (1983) (see their Table 3 and Fig. 1). These authors found that natural andesite melt with an initial P₂O₅ of 0.25 wt % lost all phosphorus after 70 h at 1,359 °C. More data are required to construct a complete model of P evaporation from silicate melts, similar to what Sugawara (1999) has suggested for Na loss from experimental charges.

SiO₂, TiO₂, and P₂O₅ components: efficiency of network-forming cations in decreasing the Fe³⁺/Fe²⁺ ratio.

On Fig. 5, we plotted Fe³⁺/Fe²⁺ ratio as a function of (SiO₂ + TiO₂). At constant temperature, both DAFT and DAFST compositions lie on the same regression line, implying that adding SiO₂ and TiO₂ roughly equally decreases ferric/ferrous ratio.

Following Sack’s et al. (1980) model, we approximated log ferric/ferrous of all experimental glasses as a linear function of the reciprocal absolute temperature and mole fractions of SiO₂, TiO₂, and P₂O₅, taking into account that only these four parameters are variable

$$\log(X_{FeO_{1.5}}/X_{FeO}) = 5919/T - 0.674 \cdot X_{SiO_2} - 0.673 \cdot X_{TiO_2} - 4.377 \cdot X_{P_{2O_5}} - 2.734 \tag{10}$$

The high value of *R*² = 0.988 shows that Eq. (10) is successful to model to the experimental dataset with a good accuracy. The temperature slope 5,919 ± 223 (1σ) is in reasonable agreement with values for natural melts following the empirical equations of Sack et al. (1980)

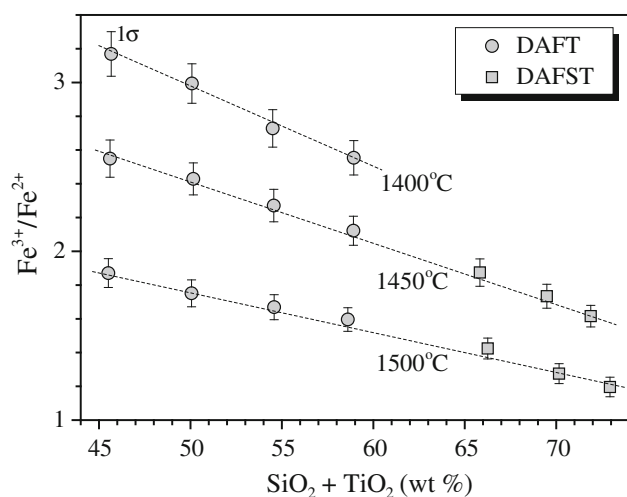


Fig. 5 Effect of $\text{SiO}_2 + \text{TiO}_2$ contents on ferric/ferrous ratio in the experimental samples

and Kilinc et al. (1983): $5,730 \pm 420$ and $5,500 \pm 390$, respectively. However, it is emphasized that the temperature effect is investigated over a range of 150 °C only.

The values of the coefficients $d_{\text{SiO}_2} = -0.674 \pm 0.037$ (1σ) and $d_{\text{TiO}_2} = -0.673 \pm 0.044$ are identical within error. This implies that adding SiO_2 and TiO_2 to a melt is equally effective (on a molar basis) in decreasing $\text{Fe}^{3+}/\text{Fe}^{2+}$ ratio. On the other hand, the value of the coefficient $d_{\text{P}_2\text{O}_5}$ of -4.377 ± 0.113 (1σ) is much lower than that of d_{SiO_2} or d_{TiO_2} . This implies that adding P_2O_5 to a melt is much more efficient in decreasing $\text{Fe}^{3+}/\text{Fe}^{2+}$ ratio than adding silica or titania.

The form of Eq. (10) implies that the relative effect of any two components on the $\text{Fe}^{3+}/\text{Fe}^{2+}$ ratio is given by the difference in those empirical coefficients, d_i . Indeed, from Eq. (10), it can be deduced that $\Delta \log(X_{\text{FeO}_{1.5}}/X_{\text{FeO}})$ at exchanging 10 mol % SiO_2 in a melt by 10 mol % P_2O_5 is equal to $(d_{\text{P}_2\text{O}_5} - d_{\text{SiO}_2})/10 = -0.37$. Such an effect is equivalent to a decrease in oxygen fugacity by approximately 1.5 log unit, assuming a slope of $\log(X_{\text{FeO}_{1.5}}/X_{\text{FeO}})$ versus $\log f_{\text{O}_2}$ to have an ideal value of 0.25.

Thus, the present finding ranks the efficiency of network-forming oxides to decrease the ferric/ferrous ratio in $\text{CaO-MgO-FeO-Fe}_2\text{O}_3\text{-SiO}_2\text{-TiO}_2\text{-P}_2\text{O}_5$ melts in the following order: $\text{P}_2\text{O}_5 \gg \text{TiO}_2 \approx \text{SiO}_2$.

A comparison with the published data

Experiments with TiO_2 -bearing compositions

Matsuzaki and Ito (1997) conducted experiments in ternary $\text{FeO-TiO}_2\text{-SiO}_2$ melts, resembling slag compositions, with $\text{TiO}_2/\text{SiO}_2$ (wt) varying from 0.5 to 2. These experiments

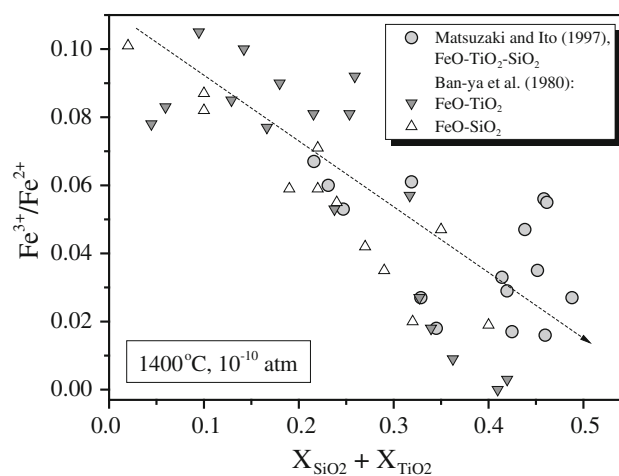


Fig. 6 Effect of $\text{SiO}_2 + \text{TiO}_2$ contents on ferric/ferrous ratio in simple slags in equilibrium with metallic iron at 1,400 °C. Experimental data from Ban-ya et al. (1980) and Matsuzaki and Ito (1997) recalculated to a constant $f_{\text{O}_2} = 10^{-10}$ atm

were carried out in equilibrium with metallic iron and f_{O_2} was buffered with H_2/CO_2 gas mixtures. The authors used their own data obtained at 1,400 °C along with the similar data of Ban-ya et al. (1980) in FeO-TiO_2 and FeO-SiO_2 binaries to plot $\text{Fe}^{3+}/\text{Fe}^{2+}$ versus $X_{\text{TiO}_2} + X_{\text{SiO}_2}$ (Fig. 2 in Matsuzaki and Ito 1997). We additionally recalculated $\text{Fe}^{3+}/\text{Fe}^{2+}$ ratio in these slags to a constant oxygen fugacity of 10^{-10} atm (an ideal slope $k = 0.25$ of $\log \text{Fe}^{3+}/\text{Fe}^{2+}$ vs. $\log f_{\text{O}_2}$ was assumed) in attempt to minimize the data scattering. The results are shown on Fig. 6. The scattering is still large and reflects perhaps problems in the accuracy of the $\text{Fe}^{3+}/\text{Fe}^{2+}$ determination at these extremely low f_{O_2} conditions where ferric content in the slags is very small. Nevertheless, the trend is evident: there is a decrease in the ferric/ferrous ratio with increasing $\text{SiO}_2 + \text{TiO}_2$ with approximately equal effects of SiO_2 and TiO_2 .

Alberto et al. (1992) studied redox equilibria in more complex $\text{CaO-TiO}_2\text{-SiO}_2$ melts modified either with 5 or 15 wt % Fe_2O_3 total at 1,500 °C in air. Experimental data were not tabulated but plotted as $\text{Fe}^{3+}/\Sigma\text{Fe}$ versus $\text{Ti}/(\text{Ti} + \text{Si})$ (Fig. 2 in Alberto et al. 1992). For the same Fe_2O_3 total, the most polymerized melts (more silicic, $\text{NBO}/\text{T} = 1.2$, $X_{\text{SiO}_2} + X_{\text{TiO}_2} \approx 0.63$ in iron-free matrix) display much lower $\text{Fe}^{3+}/\Sigma\text{Fe}$ ratio than less polymerized melts (more basic, $\text{NBO}/\text{T} = 2$, $X_{\text{SiO}_2} + X_{\text{TiO}_2} \approx 0.51$ in iron-free matrix), similar to our results obtained with the DAFST and DAFT series. The exchange of Si by Ti is either negligible in terms of $\text{Fe}^{3+}/\text{Fe}^{2+}$ (series MIN(I-VI)F5) or results in a slight oxidation of iron (e.g., series CS(VII-XV)F5, see Fig. 2 in Alberto et al. 1992).

Summarizing, increasing both SiO_2 and TiO_2 results in a decrease in the $\text{Fe}^{3+}/\text{Fe}^{2+}$ ratio in simple slags and complex silicate melts, with TiO_2 tending to be either equally

(like in present experiments) or slightly less effective in comparison with SiO_2 . This observation is in agreement with structural studies indicating that at least part of the Ti incorporated in silicate melts is in fourfold coordination as Si (e.g., Dingwell et al. 1994; Farges et al. 1996; Henderson et al. 2002). However, part of the Ti may also be five- and sixfold coordinated.

Experiments with P_2O_5 -bearing compositions

Toplis et al. (1994) investigated the effects of phosphorus on $\text{Fe}^{3+}/\text{Fe}^{2+}$ ratio in synthetic ferro-basaltic compositions. They revealed, for example, that at air conditions and fixed temperature of 1,446 and 1,545 °C, the ferric/ferrous ratio decreases by a factor of 1.3 as a result of the addition of 9.5 wt % P_2O_5 (4.4 mol %) to the initial P-free composition (see Table 2 and Fig. 1 in Toplis et al. 1994). This decrease is very similar to that observed in the present study. Note that Toplis et al. (1994) were the first who concluded that the incorporation of a P_2O_5 term is necessary in empirical equations to calculate $\text{Fe}^{3+}/\text{Fe}^{2+}$.

Large effects of P_2O_5 on ferric/ferrous ratio, much more pronounced when compared with SiO_2 , may also be extracted from the experimental data of Turkdogan and Bills (1957) in $\text{FeO}_t\text{-SiO}_2\text{-P}_2\text{O}_5$ melts at 1,550 °C. The authors report the CO/CO_2 ratio in the buffering gas mixture [Table 1 in Turkdogan and Bills (1957)], which we converted into $f\text{O}_2$ values using the thermodynamic data of Deines et al. (1974). The $\text{Fe}^{3+}/\text{Fe}^{2+}$ ratios in these slags (49 experiments in total) were then described as a function of $\log f\text{O}_2$, X_{SiO_2} , and $X_{\text{P}_2\text{O}_5}$ to obtain the following equation:

$$\log(X_{\text{FeO}_{1.5}}/X_{\text{FeO}}) = 0.20 \cdot \log f\text{O}_2 - 0.963 \cdot X_{\text{SiO}_2} - 3.105 \cdot X_{\text{P}_2\text{O}_5} + 0.641 \quad (11)$$

The parameter $k = 0.20 \pm 0.01$ at $\log f\text{O}_2$ is reasonably close to the ideal value of 0.25, which, together with the high correlation coefficient ($R^2 = 0.95$), demonstrates the high quality of the experiments and the appropriate form of Eq. (11). Thus, one can compare the efficiency of SiO_2 and P_2O_5 in these slags in changing ferric/ferrous ratio. The substitution of 10 mol % SiO_2 by the same amount of P_2O_5 lowers the $\log(X_{\text{FeO}_{1.5}}/X_{\text{FeO}})$ by a value of 0.21, which is equivalent to a decrease in the oxygen fugacity of ca. 0.9 log unit.

Jayasuriya et al. (2004) were the first who included phosphorus in the empirical equation proposed by Sack et al. (1980). They fitted $\ln(X_{\text{Fe}_2\text{O}_3}/X_{\text{FeO}})$ versus $\ln f\text{O}_2$, $1/T$ and mole fraction of oxides, including $X_{\text{P}_2\text{O}_5}$ (Eq. 12 in Jayasuriya et al. 2004). Converting $\ln(X_{\text{Fe}_2\text{O}_3}/X_{\text{FeO}})$ into $\log(X_{\text{FeO}_{1.5}}/X_{\text{FeO}})$ for a correct comparison of their results with our Eqs. (10) and (11) would lead to a value of

$d_{\text{P}_2\text{O}_5} = -27.3$ (error was not given) and $d_{\text{SiO}_2} = 0$ (silica was not included in the fitting). Here, $\Delta \log(X_{\text{FeO}_{1.5}}/X_{\text{FeO}})$ after exchanging 10 mol % SiO_2 by 10 mol % P_2O_5 is equal to -2.73 corresponding to an extremely high $f\text{O}_2$ decrease by about 11 log unit, which seems unrealistic. The conclusion that the effect of phosphorus on $\text{Fe}^{3+}/\text{Fe}^{2+}$ ratio may be much less than suggested by Jayasuriya et al. (2004) is also confirmed by the comparison of two experimental series (PW and P series) made at 1,500 °C in air by Mysen (1992). In both cases, the author used a composition close to 44CaO-56SiO₂ (wt %) as a base modified with 5 wt % Fe_2O_3 . In the P series, P_2O_5 was added to the base composition and a moderate decrease in ferric/ferrous ratio was observed. In the PW series, however, phosphorus was added as $\text{Ca}_3(\text{PO}_4)_2$ and this resulted in increase in ferric/ferrous ratio (see Fig. 8 in Mysen 1992). The addition of CaO to a melt in the $\text{SiO}_2\text{-CaO-FeO}_t$ system is known to increase $\text{Fe}^{3+}/\text{Fe}^{2+}$ ratio (Kress and Carmichael 1989). Thus, the addition of three moles CaO for one mole P_2O_5 ($\text{Ca}_3(\text{PO}_4)_2 = 3\text{CaO} \cdot \text{P}_2\text{O}_5$) largely compensates the possible decrease in ferric/ferrous induced by the addition of phosphorus.

In summary, the results in this study and the most published data suggest a significant decrease in ferric/ferrous ratio with increasing of P_2O_5 content. It is worth noting however that our most SiO_2 -rich composition DAFSP09, being recalculated on P-free base, contains only about 55 wt % SiO_2 . The synthetic ferro-basalt used by Toplis et al. (1994) contains about 51 % SiO_2 . Mysen's (1992) initial composition has about 53 % SiO_2 . Finally, the SiO_2 contents of the P-containing slags of Turkdogan and Bills (1957), even after recalculation on P-free base, do not exceed 47 wt %. Thus, on the basis of the available data, a stabilizing effect of P_2O_5 on ferrous iron can be inferred only for the basic to intermediate melts. However, it is emphasized that the data from Gwinn and Hess (1993) indicate that the effect of P_2O_5 on $\text{Fe}^{3+}/\text{Fe}^{2+}$ may be the opposite in very silicic melts (>70 wt % SiO_2 , Fig. 7). Although there is a large data scatter for the K-rich compositions, the P-bearing liquids have systematically higher $\text{Fe}^{3+}/\text{Fe}^{2+}$ ratios than P-free melts, independently on the K/Al ratio (peraluminous or peralkaline). Note that the addition of only 0.5 mol % P_2O_5 at fixed K/Al ratio and SiO_2 content may increase the ferric/ferrous in a melt by a factor of 2–3. The contrasting behavior of phosphorus in very silicic and more basic melts was also noted by Ryerson (1985) who calculated SiO_2 activity coefficients (γ_{SiO_2}) in binary and ternary melts. Ryerson (1985) showed that adding P_2O_5 to SiO_2 results in a decrease in γ_{SiO_2} , even more pronounced than adding K_2O or Na_2O . In forsterite/clinoenstatite or cristoballite/clinoenstatite saturated melts, the addition of P_2O_5 results in an increase in γ_{SiO_2} .

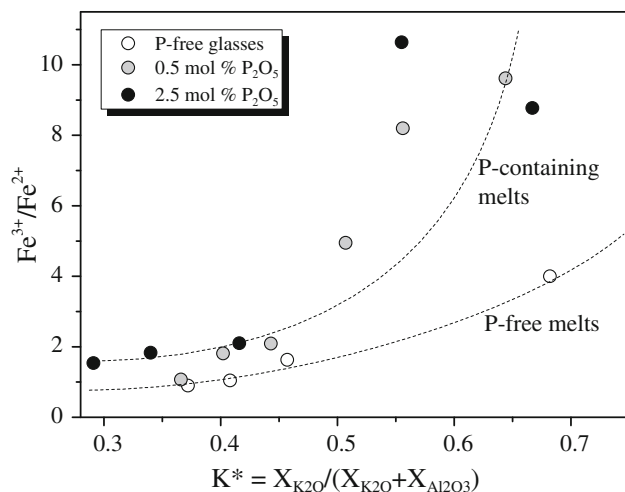


Fig. 7 Effects of K/Al ratio on $\text{Fe}^{3+}/\text{Fe}^{2+}$ in P-free, P-poor, and P-rich silicic melts at 1,400 °C in air. Experimental data from Gwinn and Hess (1993). We present three series of experiments with zero, 0.5 mol % (1.6 wt %), and 2.6 mol % (5.4 wt %) P_2O_5 (data from Tables 1, 3a, b in Gwinn and Hess 1993). All melts have approximately the same SiO_2 content (about 76 wt % \approx 85 mol %) and total Fe_2O_3 (1 mol %) but with variable K/Al ratio

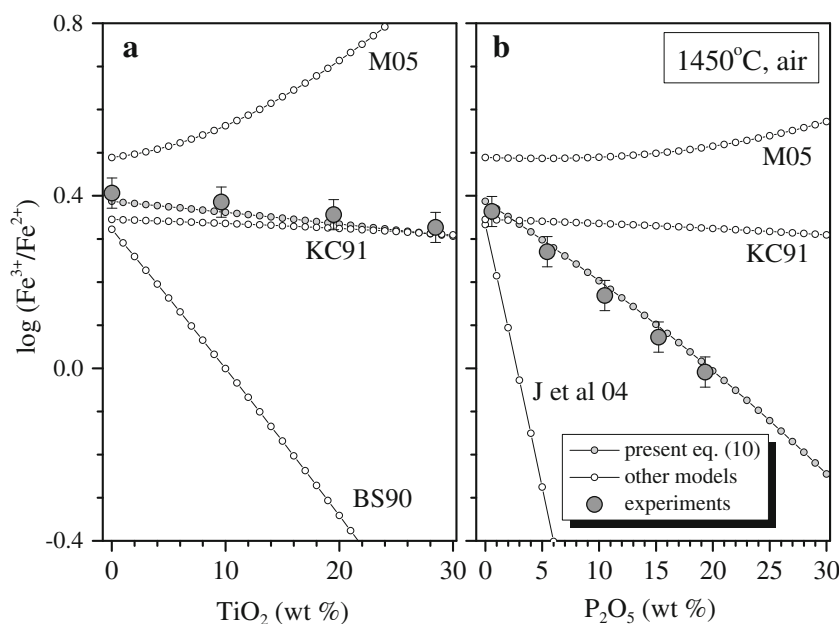
A detailed discussion of the structure of P-bearing aluminosilicate melts is out of the scope of this study, especially because structural information on the Fe-bearing compositions studied here is not available. However, the contrasting effects of P_2O_5 on the $\text{Fe}^{3+}/\text{Fe}^{2+}$ ratio in basic and felsic melts are most probably related to structural changes. Based on the experimental studies of phase relationships and applying the concepts of Korzhinskii (1959) relating mineral stability fields and melt properties, Kushiro (1975) proposed that P^{5+} could be a network former in basaltic and

intermediate melts. However, more recent studies in basic to intermediate compositions emphasized the crucial role of alkalis in alkali-rich aluminosilicate melts in forming phosphate complexes (Toplis and Dingwell 1996; Mysen and Cody 2001). It is possible that phosphate complexes may also form with alkaline-earth elements, which would apply for the compositions investigated in this study. In contrast, in more silicic compositions, part of the phosphorus can enter the network as P^{5+} charge compensated by Al^{3+} and Fe^{3+} (Gwinn and Hess 1993; Toplis and Dingwell 1996).

Empirical equations including Ti and P components

As mentioned in the introduction, most of the equations developed to predict $\text{Fe}^{3+}/\text{Fe}^{2+}$ as a function of oxygen fugacity, temperature, and melt composition ignore TiO_2 and P_2O_5 . However, a few exceptions are known. Borisov and Shapkin (1990) and Moretti (2005) included titanium oxide as a component in their equations and we compare the predictions of their models with our DAFT series at 1,450 °C in air on Fig. 8a. Jayasuriya et al. (2004; Eq. 12) and Moretti (2005) included phosphorus oxide as a component in their equations, and we compare the predictions of their models with our DAFP series at the same conditions on Fig. 8b. In both cases, calculations with Kress and Carmichael's (1991) model, where TiO_2 and P_2O_5 are not considered, are also shown. Note that the equations under discussion were calibrated on the experiments carried out mostly with natural compositions. And the differences with our experimental results obtained with model melts can be expected, but the predicted trends of $\text{Fe}^{3+}/\text{Fe}^{2+}$ versus TiO_2 or versus P_2O_5 contents may be informative.

Fig. 8 Effects of “minor” components on $\text{Fe}^{3+}/\text{Fe}^{2+}$ in melts of 10 Fe_2O_3 :90DA composition modified either with TiO_2 (a) or P_2O_5 (b) at 1,450 °C in air. A comparison of experimental results and calculation according to the published models: Moretti (2005), Kress and Carmichael (1991), Borisov and Shapkin (1990), Jayasuriya et al. (2004)



The contrasting results of Borisov and Shapkin (1990) and Moretti (2005) shown in Fig. 8a are related to the different approaches that have been used in the models. The empirical equation of Borisov and Shapkin (1990) has a form suggested by Sack et al. (1980) but with some additional complexity, the coefficients d_i and X_i are assumed to be T - fO_2 -dependent. The TiO_2 was included in the regression along with other main components and no special assumption was made. The approach of Moretti (2005) follows that suggested earlier by Ottonello et al. (2001) and is based on the concept of “thermochemical models.” These models, in addition to other important assumptions, are based on the Temkin (1945) approach, subdividing the melt structure in anion and cation sublattices. Thus, either a network-forming or network-modifying behavior should be assumed *a priori* for every melt component. Moretti (2005), following Ottonello et al. (2001), treated Ti^{4+} as a network modifier.

The trend predicted by Borisov and Shapkin (1990) shows decreasing Fe^{3+}/Fe^{2+} similar to the experimental data, but clearly overestimates the effect of TiO_2 (see Fig. 8a). The reason is that at these conditions (1,450 °C, air), d_{TiO_2} in the equation of Borisov and Shapkin (1990) is about 2.6 times higher than d_{SiO_2} (−6.3 and −2.4, respectively). Note that at lower temperature, the difference between d_{TiO_2} and d_{SiO_2} becomes lower, at 1,330 °C, they are approximately equal, and at even lower temperatures, SiO_2 is assumed to be more effective than TiO_2 in decreasing the ferric/ferrous ratio. The trend predicted by Moretti (2005) is opposite to that of the experimental results. Surprisingly, the best fit between experiments and calculations is found in Kress and Carmichael’s (1991) model, which simply ignores TiO_2 as a component affecting Fe^{3+}/Fe^{2+} ratio. The explanation is that the small decrease in ferric/ferrous ratio with increasing TiO_2 content expected by this model is simply due to a dilution effect. The equation of Kress and Carmichael (1991) includes Al_2O_3 , FeO_t , CaO , Na_2O , and K_2O as components affecting Fe^{3+}/Fe^{2+} . The alkali oxides are absent in the present melts and X_{FeO} is approximately constant since total Fe_2O_3 was fixed on the level of 10 wt %. Thus, the higher the TiO_2 content, the smaller $X_{Al_2O_3}$ and X_{CaO} in model melts are expected to be. Because $d_{Al_2O_3} = -2.243$ and $d_{CaO} = 3.201$, the Fe^{3+}/Fe^{2+} ratio in any melt with $X_{CaO} > X_{Al_2O_3}$ (like in present case) is expected to decrease with increasing concentration of additional components not included in the regression. Note that for a hypothetical melt with $X_{Al_2O_3}/X_{CaO} > |d_{CaO}/d_{Al_2O_3}| \approx 1.427$, the effect would be the opposite. In any case, for typical basaltic melts, ignoring TiO_2 seems to be the best approach.

However, this simplification is not recommended in case of P-containing melts (see Fig. 8b). The simple “dilution” effect resulting from the application of the model of Kress and Carmichael (1991) would not predict accurately the decrease in ferric/ferrous ratio with increasing P_2O_5

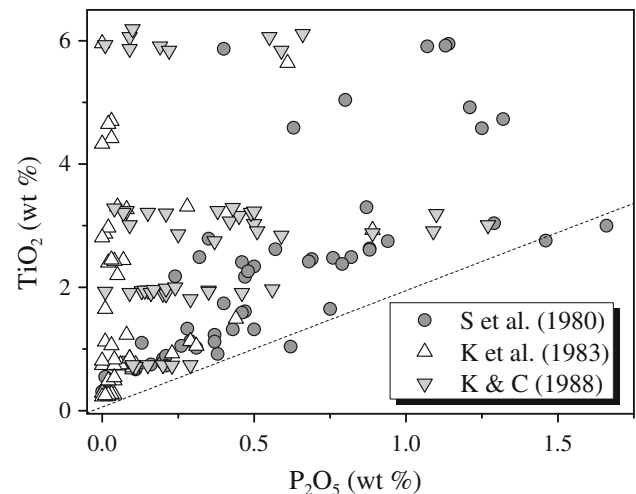


Fig. 9 TiO_2 versus P_2O_5 content in three largest datasets from experiments with natural melts: Sack et al. (1980), Kilinc et al. (1983) and Kress and Carmichael (1988)

content. As observed for TiO_2 , the trend predicted by Moretti (2005) is opposite to that observed in the experimental results. The model of Jayasuriya et al. (2004) predicts a decrease in the ferric/ferrous, but dramatically overestimates the effect of phosphorus.

On Fig. 9, we plotted TiO_2 and P_2O_5 contents in experimental glasses of three largest datasets of natural P-containing melts, which were used by Jayasuriya et al. (2004) to constrain their equation. One can note that the P-rich melts also contain large amounts of Ti. However, Jayasuriya et al. (2004) ignored titanium, following the usual practice of previous researchers. Since adding TiO_2 was demonstrated to decrease Fe^{3+}/Fe^{2+} ratio (see above), the apparent effect of P_2O_5 on ferric/ferrous ratio found by Jayasuriya et al. (2004) is most probably overestimated because it also include the effects of TiO_2 .

Implications for fO_2 determinations of MORBs

As already mentioned in the introduction, the Fe^{3+}/Fe^{2+} ratio measured in natural glasses may be used for the estimation of the redox conditions of magmas. This implies (1) an accurate determination of ferric/ferrous determination in glasses and (2) the choice of correct parameters for Eq. (4). The discussion below demonstrates that there is still a large uncertainty on the values of fO_2 deduced from the interpretation of Fe^{3+}/Fe^{2+} ratio in natural glasses to constrain the fO_2 prevailing in natural systems.

Accuracy of the determination of Fe^{3+}/Fe^{2+} ratio in natural glasses

A comprehensive review of possible wet chemical techniques and sources of error in ferric/ferrous determination

is given by Bézou and Humler (2005). In most cases, if experimental glasses are free of crystalline phase and Fe^{2+} is determined with wet chemistry (and total iron with EPMA), the $\text{Fe}^{3+}/\text{Fe}^{2+}$ ratio is considered to have an uncertainty of about 6 % (Sack et al. 1980), which propagates to a $\log f\text{O}_2$ uncertainty of about ± 0.15 . In the case of natural MORBs, however, variable amounts of plagioclase microphenocrysts or microlites in glasses may be a problem (Bézou and Humler 2005; Cottrell and Kelley 2011). Thus, choosing local techniques of ferric/ferrous determination are getting mandatory for natural samples. For example, XANES measurements may give a precision on $\text{Fe}^{3+}/\text{Fe}_t$ determination of ± 0.005 (about 3 %, Cottrell and Kelley 2011), which propagates to $\log f\text{O}_2$ precision of about ± 0.07 .

Role of compositional parameters and temperature in empirical equation

Most equations proposed in the literature reproduce the $f\text{O}_2$ of experimental dataset obtained at 1 bar with a standard error of about 0.26 log units or higher (e.g., Kress and Carmichael 1988). However, natural glasses are quench products of high-pressure melts with a pre-eruptive temperature, which is usually poorly constrained, and the absolute errors in $f\text{O}_2$ determination are expected to be higher.

To test the accuracy of the models for predicting $f\text{O}_2$ from natural glasses, Eq. (4) can be formulated as follows:

$$\log f\text{O}_2 = H/T + \log (X_{\text{Fe}_2\text{O}_3}/X_{\text{FeO}})/k - \sum d_i X_i / (k \cdot \ln 10) - c / (k \cdot \ln 10) \quad (12)$$

where $H = -h/(k \cdot \ln 10)$. For most empirical equations, H values are rather similar (e.g., $-26,251$ in Sack et al. 1980, $-25,183$ in Kilinc et al. 1983, and $-27,422$ in Jayasuriya et al. 2004) and also very close to the slope of the QFM buffer in the $\log f\text{O}_2$ versus $1/T$ diagram (e.g., $-24,442$ for the calibration of Myers and Eugster 1983). Thus, by fixing arbitrary one temperature in Eq. (12) (e.g., of $1,200$ °C for basaltic systems), the $f\text{O}_2$ of various samples relative to the QFM buffer can be estimated and compared, even when the real pre-eruptive temperatures are not known accurately (e.g., Christie et al. 1986; Bézou and Humler 2005; Cottrell and Kelley 2011). Clearly, in this case, the compositional parameter $\sum d_i X_i$ is getting especially important.

On Fig. 10 for the same set of rocks, we compare $\sum d_i X_i / (k \cdot \ln 10)$ (these values are in $\log f\text{O}_2$ units, see Eq. 12) calculated with two different models, Kilinc et al. (1983) and Kress and Carmichael (1991). A set of 103 MORB glasses analyzed by Cottrell and Kelley (2011) was chosen as an example. Although the glasses have a moderate variation in composition (they are all basalts), there is nearly no correlation between the two models. It implies that

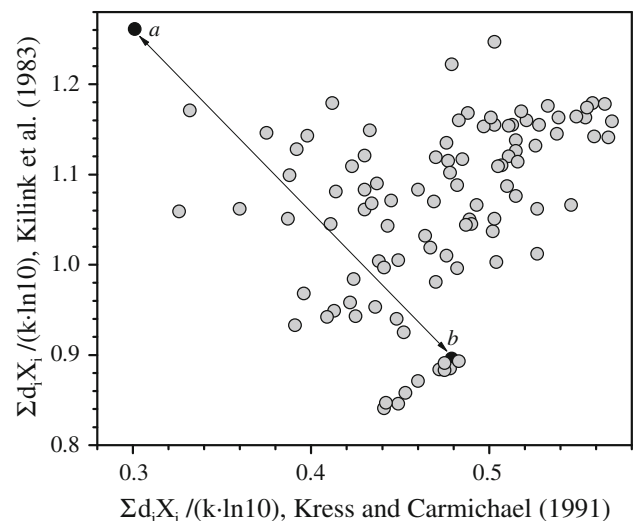


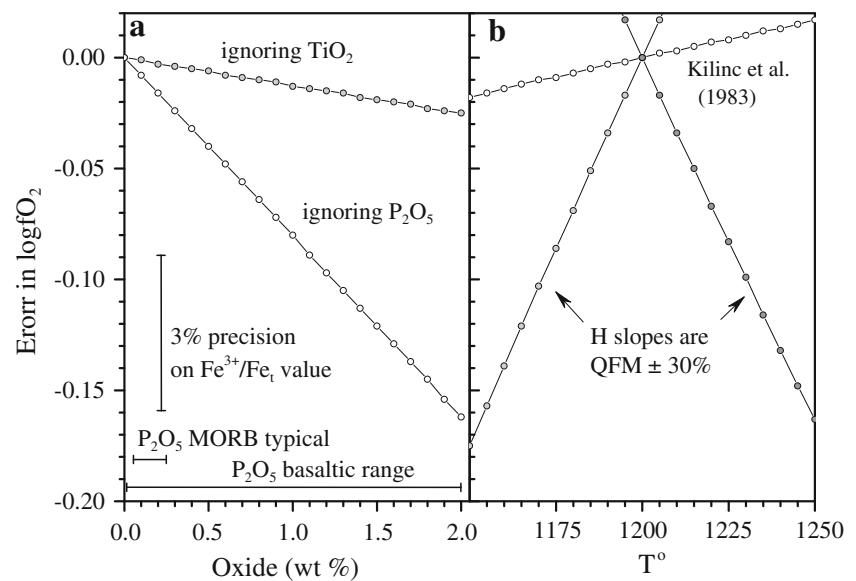
Fig. 10 A comparison of $\sum d_i X_i / (k \cdot \ln 10)$ values calculated with two different models, Kilinc et al. (1983) and Kress and Carmichael (1991), for 103 MORB glasses analyzed by Cottrell and Kelley (2011). Note that $\sum d_i X_i / (k \cdot \ln 10)$ values are in $\log f\text{O}_2$ units. Two samples *a* and *b* are chosen arbitrary to discuss the models' difference (see text for details)

conclusions drawn from a $f\text{O}_2$ variation observed for a given dataset with one model will not necessarily be confirmed with another one. For example, two arbitrary samples (*a* and *b*) are marked on Fig. 10. Let us assume them to have the same ferric/ferrous ratio. If the $f\text{O}_2$ of these samples is calculated with Kress and Carmichael's (1991) model, the sample *b* would be ~ 0.2 log unit more reduced than sample *a*. On the other hand, Kilinc's et al. (1983) model would indicate that sample *b* is ~ 0.4 log unit more oxidized than sample *a*.

Additional problems may arise by ignoring minor components in the empirical equation. On Fig. 11a, we plotted the difference between $f\text{O}_2$ calculated without taking TiO_2 or P_2O_5 and $f\text{O}_2$ calculated considering the role of TiO_2 or P_2O_5 . As mentioned above, the effect of TiO_2 is not significant, but the effect of P_2O_5 is more pronounced. The phosphorus variation in the range typical for MORB (0.05–0.25 wt % P_2O_5 , Konzett and Frost 2009) is equivalent to 0.7 % variation in $\text{Fe}^{3+}/\text{Fe}_t$, which is below the precision of the $\text{Fe}^{3+}/\text{Fe}_t$ determination in glasses. However, P_2O_5 variation of 2 wt % as observed for other basalts will be equivalent to about 7 % variation in $\text{Fe}^{3+}/\text{Fe}_t$, which would propagate to an error of 0.16 $\log f\text{O}_2$.

Other minor problems in $f\text{O}_2$ recalculation may arise if the pre-eruptive temperature of basaltic glasses differs from conventional $1,200$ °C and if the temperature slope H of these glasses differs from QFM slope (Fig. 11b). As mentioned above, H value estimated by Kilinc et al. (1983) has only a minimal deviation from the QFM buffer slope and the resulting $f\text{O}_2$ errors will not exceed 0.02 log unit

Fig. 11 Possible errors of fO_2 determination, **a** if TiO_2 or P_2O_5 is ignored, **b** if temperature slope differs from QFM buffer



when the difference between conventional 1,200 °C and real temperature does not exceed 50 °C (see Fig. 11b). Other equations show slightly higher but comparable errors. However, all these equations are statistically derived and a similar temperature slope for all compositions is assumed *a priori*. This is not the necessary case, and identical values for H for all melt compositions would be surprising. For example, Sato and Wright (1966) directly measured fO_2 in a few boreholes drilled in tholeiitic basalts through the crust of Makaopuhi lava lake, Kilauea Volcano, Hawaii. They found that $\log fO_2$ changes linearly with the reciprocal absolute temperature, with slopes varying from $-18,600$ to $-21,900$. Assuming that measured fO_2 values reflect fO_2 of cooling basalt, the corresponding H slope is 11–31 % lower than that of QFM buffer. On the other hand, a slope of $-41,327$ can be calculated for a phonotephritic composition from the data given by Moore et al. (1995, composition MAS-49), which is about 70 % higher than that of the QFM buffer. More examples and the detailed discussion on the effect of temperature on the Fe^{3+}/Fe^{2+} ratio in model and natural melts can be found in Borisov and McCammon (2010).

Figure 11b shows to which extent the calculated fO_2 may change as a function of temperature if the H value differs from that of QFM by +30 % and -30 % ($-31,775$ and $-17,109$). A difference of 50 °C between conventional 1,200 °C and real pre-eruptive temperature results in fO_2 error of about 0.17 log units.

Conclusions

1. At constant temperature, the increase in TiO_2 or P_2O_5 content in synthetic DA- Fe_2O_3 - $TiO_2/P_2O_5 \pm SiO_2$

compositions (DA represents the eutectic of the system Diopside-Anorthite) results in a decrease in the ferric/ferrous ratio both in basic and silicic melts. The effects of TiO_2 and SiO_2 on Fe^{3+}/Fe^{2+} are mostly identical. In contrast, adding P_2O_5 was found to decrease ferric/ferrous much more effectively than adding silica. Thus, the efficiency of network-forming oxides to decrease the ferric/ferrous ratio may be ranked in the following order: $P_2O_5 \gg TiO_2 \approx SiO_2$.

2. A comparison of our results with the predictions from the published empirical equations demonstrates that the effects of TiO_2 are minor and that the formulation of Kress and Carmichael (1991) is sufficient to account (indirectly) for the role of TiO_2 on Fe^{3+}/Fe^{2+} ratio in terrestrial basaltic melts. In contrast, the effects of P_2O_5 should be taken into account in new formulations to better describe its role on the ferric/ferrous ratio in natural basaltic melts.
3. An average ΔQFM value for MORB compositions may be estimated with reasonably good accuracy (ca. 0.3 log unit) if the ferric/ferrous ratio in glasses is determined with an uncertainty of ± 3 % relative. The concentration of P_2O_5 is low and will not affect significantly the fO_2 estimations. However, our present knowledge and published empirical equations do not allow us to account correctly for the effect of compositional changes on fO_2 determination.

Acknowledgments The stay of AB in Hannover was funded by the German Science Foundation (DFG, projects Ho 1337/24-1, Ho 1337/27-1 and Ho 1337/30-1). We thank Eric Wolff for the electron microprobe assistance and Anika Husen and Franziska Adams for the help in the determination of ferric/ferrous ratios in glasses. We are grateful to editor Jochen Hoefs and to the anonymous reviewers for

their comments and suggestions that allowed us to improve the paper. We are also thankful to Fabrice Gaillard for his comments on an early version of this manuscript.

References

- Alberto HV, Gil JM, Ayres de Campos N, Mysen BO (1992) Redox equilibria of iron in Ti-bearing calcium silicate quenched glasses. *J Non-Crystalline Solids* 151:39–50
- Auwera JV, Longhi J (1994) Experimental study of a jotunite (hypersthene monzodiorite): constraints on the parent magma composition and crystallization conditions (P, T, fO_2) of the Bjerkreim-Sokndal layered intrusion (Norway). *Contrib Mineral Petrol* 118:60–78
- Ban-ya S, Chiba A, Hirosaka A (1980) Thermodynamics of $Fe_xO-M_xO_y$ ($M_xO_y = CaO, SiO_2, TiO_2$ and Al_2O_3) binary melts in equilibrium with solid iron. *Tetsu-to-Hagane* 66:1484–1493
- Basaltic Volcanism Study Project (1981) Basaltic Volcanism on the Terrestrial Planets. Pergamon Press Inc., New York, p 300
- Berry AJ, Shelley MG, Foran GJ, O'Neill HStC, Scott DR (2003) A furnace design for XANES spectroscopy of silicate melts under controlled oxygen fugacity and temperatures to 1,773 K. *J Synchrotron Radiation* 10:332–336
- Bézos A, Humler E (2005) The $Fe^{3+}/\sum Fe$ ratio of MORB glasses and their implications for mantle melting. *Geochim Cosmochim Acta* 69:711–725
- Borisov A (2001) Loop technique: dynamic of metal/melt equilibration. *Min Petrol* 71:87–94
- Borisov AA (2010) Ferric-ferrous ratio in liquid iron oxides: analysis and applications to natural basaltic melts. *Petrology* 18:471–481
- Borisov AA (2012) The Ti^{4+}/Ti^{3+} ratio of magmatic melts: application to the problem of the reduction of lunar basalts. *Petrology* 20:391–398
- Borisov AA (2013) Mutual interaction of redox pairs in silicate melts: $V^{5+}/V^{4+}/V^{3+}/V^{2+}$ tetrad and other equilibria. *Petrology* 21:305–315
- Borisov A, McCammon C (2010) The effect of silica on ferric/ferrous ratio in silicate melts: an experimental investigation using Mössbauer spectroscopy. *Am Mineral* 95:545–555
- Borisov AA, Shapkin AI (1990) A new empirical equation relating Fe^{3+}/Fe^{2+} in magmas to their composition, oxygen fugacity, and temperature. *Geochem Int* 27:111–116
- Christie DM, Carmichael ISE, Langmuir CH (1986) Oxidation state of mid-ocean ridge basalt glasses. *Earth Planet Sci Lett* 79:397–411
- Corrigan G, Gibb FGF (1979) The loss of Fe and Na from a basaltic melt during experiments using the wire-loop method. *Mineral Mag* 43:121–126
- Cottrell E, Kelley KA (2011) The oxidation state of Fe in MORB glasses and the oxygen fugacity of the upper mantle. *Earth Planet Sci Lett* 305:270–282
- Cottrell E, Kelley KA (2013) Redox heterogeneity in mid-ocean ridge basalts as a function of mantle source. *Science* 340:1314–1317
- Deines PS, Nafziger RH, Ulmer GC, Woermann E (1974) Temperature-oxygen fugacity tables for selected gas mixtures in the system C-H-O at one atmosphere total pressure. *Bull Earth Mineral Sciences, Experimental Station, No 88*. Pennsylvania State University, USA
- Dingwell DB, Paris E, Seifert F, Mottana A, Romano C (1994) X-ray absorption study of Ti-bearing silicate glasses. *Phys Chem Miner* 21:501–509
- Donaldson CH, Williams RJ, Lofgren G (1975) A sample holding technique for study of crystal growth in silicate melts. *Am Mineral* 60:324–326
- Farges F, Brown GE, Navrotsky A, Gan H, Rehr JJ (1996) Coordination chemistry of Ti(IV) in silicate glasses and melts: II. Glasses at ambient temperature and pressure. *Geochim Cosmochim Acta* 60:3039–3053
- Gwinn R, Hess PC (1993) The role of phosphorus in rhyolitic liquids as determined from the homogeneous iron redox equilibrium. *Contrib Mineral Petrol* 113:424–435
- Henderson GS, Liu X, Fleet ME (2002) A Ti L-edge X-ray absorption study of Ti-silicate glasses. *Phys Chem Minerals* 29:32–42
- Jayasuriya KD, O'Neil HStC, Berry A, Campbell SJ (2004) A Mössbauer study of the oxidation state of Fe in silicate melts. *Am Mineral* 89:1597–1609
- Johnston WD (1965) Oxidation-reduction equilibria in molten $Na_2O-2SiO_2$ glass. *J. Americ Ceram Society* 48:184–190
- Kilinc A, Carmichael ISE, Rivers ML, Sack RO (1983) The ferric-ferrous ratio of natural silicate liquids equilibrated in air. *Contrib Mineral Petrol* 83:136–140
- Konzett J, Frost DJ (2009) The high P-T stability of hydroxyl-apatite in natural and simplified MORB—an experimental study to 15 GPa with implications for transport and storage of phosphorus and halogens in subduction zones. *J Petrol* 50:2043–2062
- Korzhinskii DS (1959) Acid-basic interaction of the components in silicate melts and the direction of the cotectic lines. *Acad Sci USSR Earth Sci Sec* 128:821–823
- Kress VC, Carmichael ISE (1988) Stoichiometry of the iron oxidation reaction in silicate melts. *Am Mineral* 73:1267–1274
- Kress VC, Carmichael ISE (1989) The lime-iron-silicate melt system: redox and volume systematics. *Geochim Cosmochim Acta* 53:2883–2893
- Kress VC, Carmichael ISE (1991) The compressibility of silicate liquids containing Fe_2O_3 and the effect of composition, temperature, oxygen fugacity and pressure on their redox states. *Contrib Mineral Petrol* 108:82–92
- Kushiro I (1975) On the nature of silicate melt and its significance in magma genesis; regularities in the shift of the liquidus boundaries involving olivine, pyroxene, and silica minerals. *Am J Sci* 275:411–431
- Lahiri D, Mukherjee B, Majumdar RN (1974) Mechanismus der wechselwirkung zweier redox-oxide in glass. *Glastech Berichte* 47:4–9
- Lange RA, Carmichael ISE (1989) Ferric/ferrous equilibria in $Na_2O-FeO-Fe_2O_3-SiO_2$ melts: effects of analytical techniques on derived partial molar volumes. *Geochim Cosmochim Acta* 53:2195–2204
- Matsuzaki K, Ito K (1997) Thermodynamics of $Fe_xO-TiO_2-SiO_2$ melts in equilibrium with solid iron. *ISIJ Int* 37:562–565
- Momokawa H, Sano N (1982) The effect of oxygen potential on phosphorus in the $CaO-Al_2O_3$ System. *Metall Transactions* 13B:643–644
- Moore G, Richter K, Carmichael ISE (1995) The effect of dissolved water on the oxidation state of iron in natural silicate liquids. *Contrib Mineral Petrol* 120:170–179
- Moretti R (2005) Polymerization, basicity, oxidation state and their role in ionic modeling of silicate melts. *Annals of Geophysics* 48:583–608
- Myers J, Eugster HP (1983) The system Fe-Si-O: oxygen buffer calibrations to 1500 K. *Contrib Mineral Petrol* 82:75–90
- Mysen BO (1992) Iron and phosphorus in calcium silicate quenched melts. *Chem Geol* 98:175–202
- Mysen BO, Cody GD (2001) Silicate-phosphate interactions in silicate glasses and melts: II. Quantitative, high-temperature structure of P-bearing alkali aluminosilicate melts. *Geochim Cosmochim Acta* 65:2413–2431
- Nikolaev GS, Borisov AA, Ariskin AA (1996) New fO_2 -barometers for quenched glasses of various petrochemical series. *Geochem Int* 34:753–756

- Ottonello G, Moretti R, Marini L, Zuccolini MV (2001) Oxidation state of iron in silicate glasses and melts: a thermochemical model. *Chem Geol* 174:157–179
- Palme H, O'Neill HStC (2003) Geochemical estimates of mantle composition, in *Treatise on Geochemistry*. Vol 2. Ed. R.W. Carlson, Elsevier, Oxford, 1–38
- Pik R, Deniel C, Coulon C, Yirgu G, Hofmann C, Ayalew D (1998) The northwestern Ethiopian plateau flood basalts: classification and spatial distribution of magma types. *J. Volcanol Geotherm Research* 81:91–111
- Pretorius EB, Snellgrove R, Muan A (1992) Oxidation state of chromium in $\text{CaO-Al}_2\text{O}_3\text{-CrO}_x\text{-SiO}_2$ melts under strongly reducing conditions at 1,500°C. *J Am Ceram Soc* 75:1378–1381
- Roeder PL, Emslie RF (1970) Olivine-liquid equilibrium. *Contrib Mineral Petrol* 29:275–289
- Russell C (1989) Redox reactions during cooling of glass melts. *Glass Science Technol* 62:199–203
- Ryerson FJ (1985) Oxide solution mechanisms in silicate melts: systematic variations in the activity coefficients of SiO_2 . *Geochim Cosmochim Acta* 49:637–649
- Sack RO, Carmichael ISE, Rivers ML, Ghiorso MS (1980) Ferric-ferrous equilibria in natural silicate liquids at 1 bar. *Contrib Mineral Petrol* 75:369–376
- Sato M, Wright TL (1966) Oxygen fugacities directly measured in magmatic gases. *Sciences* 153:1103–1105
- Schreiber HD, Haskin LA (1976) Chromium in basalts: experimental determination of redox states and partitioning among synthetic silicate phases. *Proceedings 7th Lunar Sci Conf*:1221–1259
- Schreiber HD, Thanyasiri T, Lach JJ, Legere RA (1978) Redox equilibria of Ti, Cr, and Eu in silicate melts: reduction potentials and mutual interactions. *Physics Chem Glasses* 19:126–139
- Schreiber HD, Peters LJ, Beckman JW, Schreiber CW (1996) Redox chemistry of iron-manganese and iron-chromium interactions in soda lime silicate glass melts. *Glastech Ber Glass Sci Technol* 69:269–277
- Schuessler JA, Botcharnikov RE, Behrens H, Misiti V, Freda C (2008) Oxidation state of iron in hydrous phono-tephritic melts. *Am Mineral* 93:1493–1504
- Sugawara T (1999) Experimental techniques to minimize Fe and Na losses in one atmosphere gas mixing furnace. *J Min Petrol Econ Geology* 94:425–441
- Tangeman JA, Lange R, Forman L (2001) Ferric-ferrous equilibria in $\text{K}_2\text{O-FeO-Fe}_2\text{O}_3\text{-SiO}_2$ melts. *Geochim Cosmochim Acta* 65:1809–1819
- Temkin M (1945) Mixtures of fused salts as ionic solutions. *Acta Phys Chim URSS* 20:411–420
- Thorber CR, Roeder PL, Foster JR (1980) The effect of composition on the ferric-ferrous ratio in basaltic liquids at atmospheric pressure. *Geochim Cosmochim Acta* 44:525–532
- Toplis MJ (2005) The thermodynamics of iron and magnesium partitioning between olivine and liquid: criteria for assessing and predicting equilibrium in natural and experimental systems. *Contrib Mineral Petrol* 149:22–39
- Toplis MJ, Dingwell DB (1996) The variable influence of P_2O_5 on the viscosity of melts of differing alkali/aluminium ratio: implications for the structural role of phosphorus in silicate melts. *Geochim Cosmochim Acta* 60:4107–4121
- Toplis MJ, Dingwell DB, Libourel G (1994) The effect of phosphorus on the iron redox ratio, viscosity, and density of an evolved ferro-basalt. *Contrib Mineral Petrol* 117:293–304
- Tsuyuhara A, Nagahara H, Hushiro I (1981) Volatilization of sodium from silicate melt spheres and its application to the formation of chondrules. *Geochim Cosmochim Acta* 45:1357–1367
- Turkdogan ET, Bills PM (1957) A Thermodynamic Study of $\text{FeO-Fe}_2\text{O}_3\text{-SiO}_2$, $\text{FeO-Fe}_2\text{O}_3\text{-P}_2\text{O}_5$ and $\text{FeO-Fe}_2\text{O}_3\text{-SiO}_2\text{-P}_2\text{O}_5$ Molten Systems. *J Iron Steel Inst* 186:329–339
- Watson EB (1980) Apatite and phosphorus in mantle source region: an experimental study of apatite/melt equilibria at pressures to 25 kbar. *Earth Planet Sci Lett* 51:322–335
- Wilson AD (1960) The micro-determination of ferrous iron in silicate minerals by a volumetric and a colorimetric method. *Analyst* 85:823–827